

# Laboratory confirmation of $C_{60}^+$ as the carrier of two diffuse interstellar bands

E. K. Campbell<sup>1</sup>, M. Holz<sup>1</sup>, D. Gerlich<sup>2</sup> & J. P. Maier<sup>1</sup>

The diffuse interstellar bands are absorption lines seen towards reddened stars<sup>1</sup>. None of the molecules responsible for these bands have been conclusively identified<sup>2</sup>. Two bands at 9,632 Ångströms and 9,577 Ångströms were reported in 1994, and were suggested to arise from  $C_{60}^+$  molecules (ref. 3), on the basis of the proximity of these wavelengths to the absorption bands of  $C_{60}^+$  measured in a neon matrix<sup>4</sup>. Confirmation of this assignment requires the gas-phase spectrum of  $C_{60}^+$ . Here we report laboratory spectroscopy of  $C_{60}^+$  in the gas phase, cooled to 5.8 kelvin. The absorption spectrum has maxima at  $9,632.7 \pm 0.1$  Ångströms and  $9,577.5 \pm 0.1$  Ångströms, and the full widths at half-maximum of these bands are  $2.2 \pm 0.2$  Ångströms and  $2.5 \pm 0.2$  Ångströms, respectively. We conclude that we have positively identified the diffuse interstellar bands at 9,632 Ångströms and 9,577 Ångströms as arising from  $C_{60}^+$  in the interstellar medium.

Shortly after the discovery of  $C_{60}$  (ref. 5), the question of its relevance to the diffuse interstellar bands (DIBs) was raised<sup>6</sup>. It soon became apparent that neutral  $C_{60}$  does not have the appropriate absorptions in the DIB range<sup>7</sup>. However, owing to its low ionization potential, it was pointed out<sup>8</sup> that  $C_{60}$  would be present mainly as  $C_{60}^+$  in the diffuse interstellar clouds and hence could be a DIB carrier. Charge transfer complexes of  $(C_{60}\text{-M})^+$ , where M is any cosmically abundant atom, have also been considered and proposed as further candidates<sup>8</sup>. With the discovery of  $C_{60}$  in planetary<sup>9</sup> and reflection nebula<sup>10</sup>, interest in  $C_{60}^+$  has been renewed.

We built an apparatus to measure the electronic spectra of cations that are of astrophysical interest at temperatures that are typical of the interstellar medium<sup>11</sup>. The central part of the instrument is a cryogenic 22-pole radio-frequency trap<sup>12</sup>, in which ions are confined and undergo collisions with cold (5 K) and very dense ( $4 \times 10^{15} \text{ cm}^{-3}$ ) helium. In the case of smaller polyatomic cations, we were able to show spectroscopi-

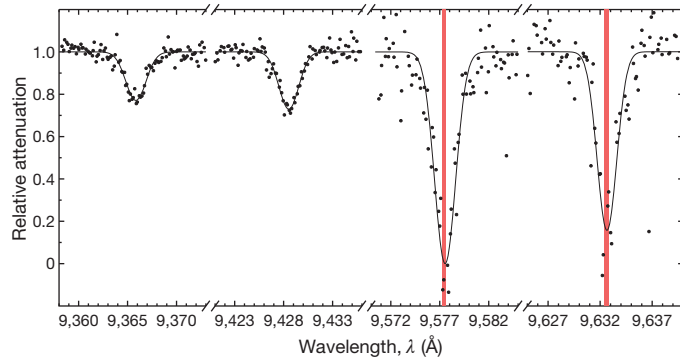


**Figure 1 | Gas-phase laboratory spectra of  $C_{60}^+$  at 5.8 K.** The spectra were recorded by monitoring the depletion on the  $C_{60}^+$ -He mass channel but, as described in the text, the effect of the helium is so small (less than 0.2 Å) that they can be considered as  $C_{60}^+$  spectra for comparison with astronomical data. Gaussian fits to the experimental data (circles) are represented by the solid black lines. The intensities of the bands have been scaled by the measured relative absorption cross-sections. The fit parameters are given in Table 1. The vertical red lines are the rest wavelengths,  $9,577.4 \pm 0.2$  Å and  $9,632.6 \pm 0.2$  Å, of two reported DIBs<sup>17</sup>; their widths represent the uncertainty.

cally that there are a sufficient number of collisions to ensure that the rotational and vibrational temperatures are equilibrated<sup>13</sup>. Under these conditions it became possible to synthesize *in situ* helium complexes of mass-selected ions via ternary association<sup>14</sup>.

These experimental advances allowed us to obtain the electronic spectrum of  $C_{60}^+$ -He by one-photon excitation followed by the loss of the helium atom. Such methods have been used for decades in spectroscopy of ions, mainly in the infrared<sup>15</sup> using rare gases, but also in the visible with helium attachment<sup>16</sup>. Owing to the low binding energies of weakly bound complexes such as  $C_{60}^+$ -He, temperatures below 8 K are required.

The measured spectra of  $C_{60}^+$ , presented in Fig. 1, are in very close agreement with the two DIBs at 9,632 Å and 9,577 Å. As is expected from the weak interaction of the helium, measurement of the corresponding absorption for  $C_{60}^+$ -He<sub>2</sub> (Fig. 2) indicates that the shift on the electronic transition is less than 0.2 Å.

The best fits to our data with a single function are obtained using a Gaussian function, rather than a Lorentzian. The band maxima are at  $9,632.7 \pm 0.1$  Å and  $9,577.5 \pm 0.1$  Å. The rest wavelengths for the DIBs are  $9,632.6 \pm 0.2$  Å and  $9,577.4 \pm 0.2$  Å after correction for stellar lines<sup>17</sup>. The extracted wavelengths towards different stars are nearly all within 1 Å of those given above<sup>17–19</sup>. This agreement with our laboratory data is remarkable, especially considering the corrections needed in the determination of the DIBs. In astronomical measurements, small differences in the wavelength of the band maximum, band full width at half-maximum (FWHM), and relative equivalent widths arise from the environmental conditions within the interstellar clouds, the number of clouds sampled in the line of sight and the accuracy of the telluric corrections.

Further support for the assignment of  $C_{60}^+$  as a DIB carrier comes from the widths of the two bands at 9,632.7 Å and 9,577.5 Å. The FWHM value of the interstellar bands that was reported following observations towards HD183143 is  $2.85 \pm 0.2$  Å (ref. 18). Our laboratory results are  $2.2 \pm 0.2$  Å and  $2.5 \pm 0.2$  Å for the maxima at  $9,632.7 \pm 0.1$  and  $9,577.5 \pm 0.1$  Å, respectively. The FWHM of the  $C_{60}^+$  rotational profile at 5.8 K is about 1 Å (ref. 20). The lines are therefore broadened by internal conversion, indicating a lifetime of 2 ps of the excited electronic state.

The somewhat larger FWHM of the DIBs is expected because of the higher rotational temperature in the diffuse clouds. Temperatures of non-polar molecules are higher than the 5.8 K in our measurements; for example,  $H_3^+$  (ref. 21) and  $C_3$  (ref. 22) lie in the 30–80 K range.

**Table 1 | Gas-phase band maxima, widths and absorption cross-sections**

$\lambda$ (Å)	FWHM (Å)	$\sigma_{\text{rel}}$
$9,632.7 \pm 0.1$	$2.2 \pm 0.2$	0.8
$9,577.5 \pm 0.1$	$2.5 \pm 0.2$	1
$9,428.5 \pm 0.1$	$2.4 \pm 0.1$	0.3
$9,365.9 \pm 0.1$	$2.4 \pm 0.1$	0.2

The wavelengths,  $\lambda$ , band FWHMs and standard deviations are determined from fits to the  $C_{60}^+$ -He fragmentation spectra using a single Gaussian function. The experimentally determined relative absorption cross-sections,  $\sigma_{\text{rel}}$ , are a measure of the relative intensities, with an estimated uncertainty of about 20%.

<sup>1</sup>Department of Chemistry, University of Basel, Klingelbergstrasse 80, CH-4056 Basel, Switzerland. <sup>2</sup>Department of Physics, Technische Universität, 09107 Chemnitz, Germany.

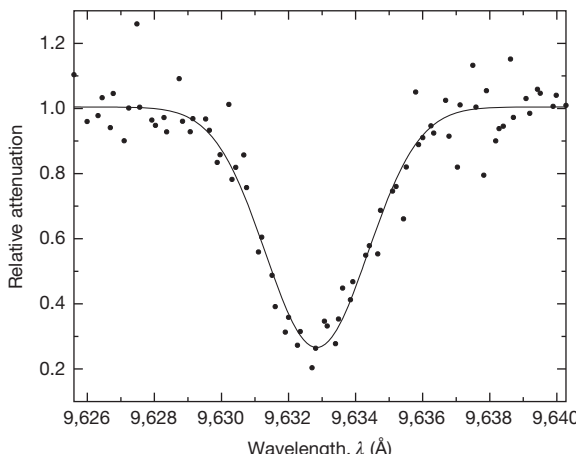


**Figure 2 |  $\text{C}_{60}^+$ -He<sub>2</sub> spectrum.** This spectrum was recorded by monitoring the depletion on the  $\text{C}_{60}^+$ -He<sub>2</sub> mass channel. A Gaussian fit to the experimental data (circles) is represented by the solid line. The fit yields a band maximum at  $9,632.8 \pm 0.1 \text{ \AA}$  and a FWHM of  $3.6 \pm 0.2 \text{ \AA}$ .

The relative cross-sections of the  $9,632.7 \pm 0.1 \text{ \AA}$  and  $9,577.5 \pm 0.1 \text{ \AA}$  laboratory absorptions were determined (Methods, Fig. 3) to be about equal, in good agreement with the intensities of the DIBs. The equivalent widths of the  $9,632 \text{ \AA}$  and  $9,577 \text{ \AA}$  DIBs vary somewhat in the literature<sup>17–19</sup>, and the  $9,632 \text{ \AA}$  DIB is partially blended with a Mg(II) line. The consensus seems to be that the equivalent widths of the DIBs are comparable, or perhaps that the equivalent width of the  $9,577 \text{ \AA}$  DIB is a bit larger.

In the study of the absorption spectrum in the neon matrix<sup>4</sup>, it was not clear what the two transitions close to the DIBs were caused by. The current experiments clarify this: irradiation at either  $9,632.7 \text{ \AA}$  or  $9,577.5 \text{ \AA}$  leads to near-complete attenuation in the number of complexes, as shown in Fig. 3. This result indicates that the two transitions arise from a single structural isomer. The implications of our findings are that both transitions originate from the lowest vibrational level of the ground electronic state,  ${}^2\text{A}_{1u}$  in  $\text{D}_{5d}$  symmetry, and result in two excited states separated by  $55.2 \text{ \AA}$ . These are either two electronic states, suggested on the basis of magnetic circular dichroism

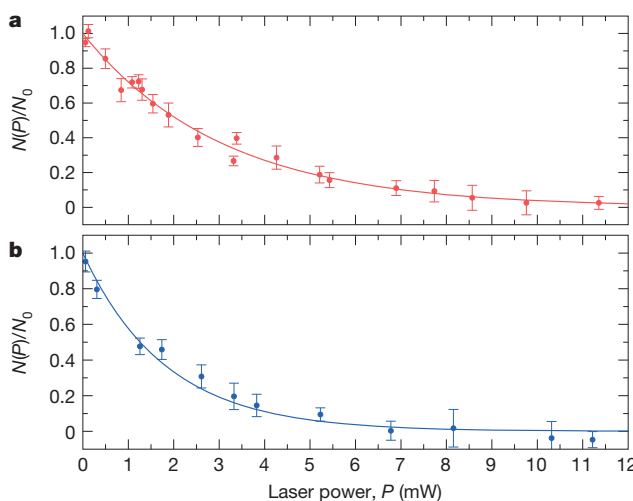


**Figure 3 | Relative cross-section measurement.** **a, b,** Depletion on the  $\text{C}_{60}^+$ -He mass channel as a function of laser power at  $9,632 \text{ \AA}$  (a) and  $9,577 \text{ \AA}$  (b).  $N(P)$  is the number of  $\text{C}_{60}^+$ -He complexes (as a function of laser power,  $P$ );  $N_0 = N(0)$ . Experimental data (circles,  $\pm 1 \text{ s.d.}$ ) were corrected for the number of background ions appearing at a mass-to-charge ratio of  $724 \text{ AMU}/e$  (for example,  ${}^{13}\text{C}_4{}^{12}\text{C}_{56}$ ). Exponential fits (solid lines, see Methods) provide information on the absorption cross-sections and indicate that all trapped ions interact with the laser.

measurements in argon matrices, or the two spin-orbit components of the upper state,  ${}^2\text{E}_g$  in  $\text{D}_{5d}$  (refs 23, 24).

According to the absorption spectrum in the neon matrix<sup>4</sup>, the next two bands on the short-wavelength side of the  $9,577 \text{ \AA}$  peak are weaker by a factor of 4–5 in intensity. A search for DIBs at  $9,366 \text{ \AA}$  and  $9,419 \text{ \AA}$  was reported<sup>17,19</sup>. In this region, we observed bands in the gas phase at  $9,365.9 \pm 0.1 \text{ \AA}$  and  $9,428.5 \pm 0.1 \text{ \AA}$ , as shown in Fig. 1. The lack of a detected DIB at  $9,366 \text{ \AA}$  was assumed to indicate an upper limit of 16% of the  $9,577 \text{ \AA}$  band intensity<sup>17</sup>. This conclusion is consistent with the relative cross-section of about 20% that we determined. The other band was not found, despite searching for it in interstellar clouds at  $9,419 \text{ \AA}$ . However, this absorption is at  $9,428.5 \pm 0.1 \text{ \AA}$  in the gas phase, according to our measurement. A ‘depression’ at  $9,428 \text{ \AA}$  was reported<sup>17</sup>. Astronomical measurements in this region are difficult because of stellar lines and telluric absorptions from water vapour.

**Online Content** Methods, along with any additional Extended Data display items and Source Data, are available in the online version of the paper; references unique to these sections appear only in the online paper.

Received 22 April; accepted 11 May 2015.

- Herbig, G.H. The diffuse interstellar bands. *Annu. Rev. Astron. Astrophys.* **33**, 19–73 (1995).
- Snow, T. P. & McCall, B. J. Diffuse atomic and molecular clouds. *Annu. Rev. Astron. Astrophys.* **44**, 367–414 (2006).
- Foing, B. H. & Ehrenfreund, P. Detection of two interstellar absorption bands coincident with spectral features of  $\text{C}_{60}^+$ . *Nature* **369**, 296–298 (1994).
- Fulara, J., Jakobi, M. & Maier, J. P. Electronic and infrared spectra of  $\text{C}_{60}^+$  and  $\text{C}_{60}^-$  in neon and argon matrices. *Chem. Phys. Lett.* **211**, 227–234 (1993).
- Kroto, H. W., Heath, J. R., O'Brian, S. C., Curl, R. F. & Smalley, R. E.  $\text{C}_{60}$ : Buckminsterfullerene. *Nature* **318**, 162–163 (1985).
- Kroto, H. W. Space, stars,  $\text{C}_{60}$ , and soot. *Science* **242**, 1139–1145 (1988).
- Herbig, G. H. The search for interstellar  $\text{C}_{60}$ . *Astrophys. J.* **542**, 334–343 (2000).
- Kroto, H. W. & Jura, M. Circumstellar and interstellar fullerenes and their analogues. *Astron. Astrophys.* **263**, 275–280 (1992).
- Cami, J., Bernard-Salas, J., Peeters, E. & Malek, S. E. Detection of  $\text{C}_{60}$  and  $\text{C}_{70}$  in a young planetary nebula. *Science* **329**, 1180–1182 (2010).
- Sellgren, K. et al.  $\text{C}_{60}$  in reflection nebulae. *Astrophys. J.* **722**, L54–L57 (2010).
- Chakrabarty, S. et al. A novel method to measure electronic spectra of cold molecular ions. *J. Phys. Chem. Lett.* **4**, 4051–4054 (2013).
- Gerlich, D. Ion-neutral collisions in a 22-pole trap at very low energies. *Phys. Scr.* **T59**, 256–263 (1995).
- Chakrabarty, S., Rice, C. A., Mazzotti, F. J., Dietsche, R. & Maier, J. P. Electronic absorption spectrum of triacetylene cation for astronomical considerations. *J. Phys. Chem. A* **117**, 9574–9577 (2013).
- Jašić, J., Žabka, J., Roithová, J. & Gerlich, D. Infrared spectroscopy of trapped molecular dications below 4 K. *Int. J. Mass Spectrom.* **354–355**, 204–210 (2013).
- Duncan, M. A. Infrared laser spectroscopy of mass-selected carbocations. *J. Phys. Chem. A* **117**, 11477–11491 (2012).
- Bieske, E. J., Soliva, A. M., Friedmann, A. & Maier, J. P. Electronic spectra of  $\text{N}_2^+(-\text{He})_n$  ( $n = 1, 2, 3$ ). *J. Chem. Phys.* **96**, 28–34 (1992).
- Jenniskens, P., Mulas, G., Porceddu, I. & Benvenuti, P. Diffuse interstellar bands near  $9600 \text{ \AA}$ : not due to  $\text{C}_{60}^+$  yet. *Astron. Astrophys.* **327**, 337–341 (1997).
- Foing, B. H. & Ehrenfreund, P. New evidences for interstellar  $\text{C}_{60}^+$ . *Astron. Astrophys.* **317**, L59–L62 (1997).
- Galazutdinov, G. A., Krelowski, J., Musaev, F. A., Ehrenfreund, P. & Foing, B. H. On the identification of the  $\text{C}_{60}^+$  interstellar features. *Mon. Not. R. Astron. Soc.* **317**, 750–758 (2000).
- Edwards, S. A. & Leach, S. Simulated rotational band contours of  $\text{C}_{60}$  and their comparison with some of the diffuse interstellar bands. *Astron. Astrophys.* **272**, 533–540 (1993).
- Indriolo, N., Geballe, T. R., Oka, T. & McCall, B. J.  $\text{H}_3^+$  in diffuse interstellar clouds: a tracer for the cosmic-ray ionization rate. *Astrophys. J.* **671**, 1736–1747 (2007).
- Maier, J. P., Lakin, N. M., Walker, G. A. H. & Bohlender, D. A. Detection of  $\text{C}_3$  in diffuse interstellar clouds. *Astrophys. J.* **553**, 267–273 (2001).
- Gasyra, Z., Andrews, L. & Schatz, P. N. Near-infrared absorption spectra of  $\text{C}_{60}$  radical cations and anions prepared simultaneously in solid argon. *J. Phys. Chem.* **96**, 1525–1527 (1992).
- Langford, V. S. & Williamson, B. E. Magnetic circular dichroism of  $\text{C}_{60}^+$  and  $\text{C}_{60}^-$  radicals in argon matrixes. *J. Phys. Chem. A* **103**, 6533–6539 (1999).

**Acknowledgements** This work was financially supported by the European Research Council (ERC-AdG-ElecSpecIons: 246998).

**Author Contributions** E.K.C., M.H. and D.G. recorded and analysed the experimental data. J.P.M. and E.K.C. wrote the paper with input from all authors. All authors discussed the results and commented on the manuscript. J.P.M. initiated and led the project.

**Author Information** Reprints and permissions information is available at [www.nature.com/reprints](http://www.nature.com/reprints). The authors declare no competing financial interests. Readers are welcome to comment on the online version of the paper. Correspondence and requests for materials should be addressed to J.P.M. (j.p.maier@unibas.ch).

## METHODS

The use of cryogenic ion traps for astrophysics and spectroscopy is well documented in the literature<sup>11–14</sup>.

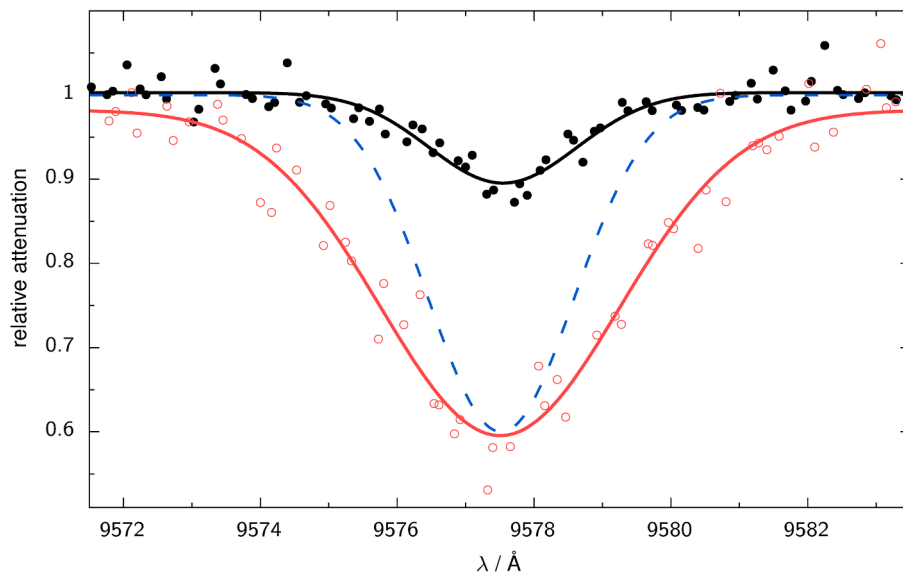
**Experimental procedure.**  $C_{60}^+$  was produced using 50 eV electron impact of the neutral gas at  $10^{-4}$  mbar. After passing through a quadrupole mass filter, operated in the transmission mode, the internally hot ions are deflected by 90 degrees using an electrostatic quadrupole bender and injected into a 22-pole radio frequency (amplitude,  $V_0 = 160$  V; frequency,  $f = 4.85$  MHz) ion trap. The use of the bender allowed for the separation of neutrals and ions. The trap is mounted onto the second stage of a closed-cycle cryostat (Sumitomo, RDK-205E). Trapping is achieved by pulsing the potential of the entrance and exit electrodes; the trap contents are analysed using a quadrupole mass spectrometer and a Daly detector. Experiments are performed at a repetition rate of 1 Hz.

The internal degrees of freedom of the ions are cooled via inelastic collisions with helium buffer gas, which is in equilibrium with the temperature of the trap walls (nominal temperature,  $T_{\text{nom}} = 5$  K). The  $C_{60}^+ - \text{He}$  ions are rotationally cold because the internal temperature of the ion ( $T_{\text{rot}}$ ) is given by the mass-weighted average of the translational temperature of the ions and the buffer gas,  $T_{\text{rot}} = (m_1 T_2 + m_2 T_1)/(m_1 + m_2)$ , where  $m_1$ ,  $T_1$  and  $m_2$ ,  $T_2$  are the mass and translational temperature of the ions and buffer gas, respectively. For heavy  $C_{60}^+ - \text{He}$  stored in cold helium, a translational temperature of 150 K for the ions still leads to a rotational temperature  $T_{\text{rot}} = 5.8$  K.

About  $10^5 C_{60}^+ \text{ cm}^{-3}$  per filling are loaded into the trap by lowering the potential of the entrance electrode for 200 ms. Here they interact with high-number-density helium buffer gas,  $[\text{He}] = 4 \times 10^{15} \text{ cm}^{-3}$ , for 500 ms. The helium is introduced by resonantly exciting a piezo valve with amplitude 4.5 V at a frequency of 3.8 kHz. In the trap,  $C_{60}^+ - \text{He}$  complexes are formed via ternary association. Owing to extremely slow cooling of all vibrational modes to their ground states, attachment of helium to primary ions is very inefficient. However, a few per cent are sufficient, especially because a large fraction can be

fragmented. After pumping out the gas for 100 ms, the ion cloud is exposed to continuous-wave radiation that is produced from a homebuilt diode laser (up to 100 mW, 12 MHz bandwidth), which is gated with a mechanical shutter and open for a period of 300 ms. To avoid power broadening, only 2 mW were used for recording the two bands at  $9,632.7 \pm 0.1$  Å and  $9,577.5 \pm 0.1$  Å. For the other two, at 9,428.5 Å and 9,365.9 Å, 20–30 mW were required to obtain an attenuation of 20%. The potential of the exit electrode is lowered, and the contents extracted and analysed 150 ms after irradiation. The resulting laser-induced attenuation of the number of complexes was monitored as a function of laser frequency, yielding photofragmentation spectra.

**Relative photo-absorption cross-sections.** In the present experiment, a confined ensemble of some thousand  $C_{60}^+ - \text{He}$  complexes,  $N(P)$ , where  $P$  is the laser power measured at the exit of the instrument, is exposed to a continuous-wave diode laser. As can be seen from Fig. 3, the effective power density in the trap (diameter of the ion cloud is 0.8 cm) can be varied over a wide range. The observed attenuation curves have been fitted with the exponential function,  $N(P) = N_0 \exp(-P/P_0)$ . The characteristic power,  $P_0$ , is a measure of the relative fragmentation cross-section of the complex. It is safe to assume that the relative fragmentation cross-section is equal to the relative absorption cross-section,  $\sigma_{\text{rel}}$  and provides a reliable value for the absorption of  $C_{60}^+$  itself. The results shown in Fig. 3 indicate that all complexes absorb at  $9,632.7 \pm 0.1$  Å or  $9,577.5 \pm 0.1$  Å. This supports the argument that, after many collisions with helium in the trap, only one structural isomer remains, as discussed in the main text. The relative cross-sections for four bands are presented in Table 1. Calculation of absolute cross-section values relies on the assumption that all ions uniformly explore the trapping volume. An attractive patch potential on one of the 22-pole electrodes, however, may cause the ions to stay outside the laser beam for longer than assumed. This leads to a large uncertainty in the absolute numbers and therefore only relative photo-absorption cross-sections are reported. The influence of power broadening is shown in Extended Data Fig. 1.



**Extended Data Figure 1 | Influence of laser power on the 9,577.5 Å band.**  
Gas-phase spectrum recorded by monitoring the depletion on the  $\text{C}_{60}^+$ -He mass channel using 1.5 mW (black) and 14 mW (red). Gaussian fits to

experimental data (circles) are represented by solid lines, and give FWHMs of  $2.5 \pm 0.2 \text{ Å}$  and  $4.1 \pm 0.2 \text{ Å}$  at 1.5 mW and 14 mW, respectively. The blue dashed line shows a Gaussian with a FWHM of  $2.5 \text{ Å}$ .